

THE FUZZY APPLICATIONS OF HOMOTOPY PERTURBATION METHOD FOR UNSTEADY MHD BOUNDARY LAYER FLOW AND HEAT TRANSFER DUE TO STRETCHING SHEET IN THE PRESENCE OF HEAT

¹K.VIJAYAKUMAR , ²K.JAYALAKSHMY

¹(Asst.prof, PG & Research Department of Mathematics , Arignar Anna Govt Arts College, Villupuram.)

²(Asst.prof, PG & Research Department of Mathematics , Arignar Anna Govt Arts College, Villupuram.)

ABSTRACT: *The Fuzzy homotopy perturbation method (HPM) is used to handle the numerical solution of fuzzy fractional predator-prey system with fuzzy initial conditions and implementations of FHPM to fuzzy fractional predator-prey equations with fuzzy initial conditions and the integral of fuzzy function, using Lebesgue type concept by Fuzzy Adomian Decomposition Method.*

Keywords: *Fuzzy Homotopy perturbation method, fuzzy adomian decomposition method, Initial conditions.*

I INTRODUCTION

The study of the flow field created by the moving surface in a quiescent fluid is relevant to several practical applications in the field of metallurgy and chemical engineering. A number of technical processes concerning polymers involve the cooling of continuous strips or filaments by drawing them through quiescent fluid. In these cases the properties of the final product depend to a great extent on the rate of cooling which governed by the structure of the boundary layer near the moving strips. Sakiadis (1931) was the first to study the boundary layer flow due to a moving continuously stretching surface in a fluid at rest. Since then different aspects of the flow past over a continuous moving surface have been investigated by different researchers under different conditions. Several investigators have studied different dimensions of the boundary layer flow of electrically conducting fluid and heat transfer due to stretching sheet in the presence of a transverse magnetic field.

The flow of an electrically conducting fluid past stretching sheet under the effect of a magnetic field has attracted the attention of many researchers in view of its wide applications in many engineering problems such as magneto hydrodynamic (MHD) generator, plasma studies, nuclear reactors, oil exploration, geothermal energy extraction, and the boundary layer control in the field of aero dynamics. Consequently, Ishak (2010) has studied unsteady laminar magneto hydrodynamic (MHD) flow and heat transfer due to continuously stretching plate immersed in an electrically conducting fluid. The result shows that heat transfer rate at the surface increases with an increase in unsteadiness parameter and Prandtl number Pr , but decreases with an increase in the values of magnetic parameter M .

Ishak et al. (2009) have analyzed the boundary-layer flow and heat transfer due to a stretching vertical surface. They discussed the effects of unsteadiness parameter, buoyancy parameter and Prandtl number on the flow and heat transfer characteristics. They indicated that the heat transfer rate at the surface increases with an increase in unsteadiness parameter, buoyancy parameter and Prandtl number. Elbashbeshy (1998) analyzed heat transfer over a stretching surface with variable surface heat flux. His result indicates that suction increases the heat transfer from the surface, where as injection causes a decrease in the heat transfer. Elbashbeshy et al. and Zheng (2010, 2011) studied heat transfer over an unsteady stretching surface in the presence of a heat source or sink. The numerical results reveal that the momentum boundary layer thickness decreases with an increase in unsteadiness parameter. However, an increase in the unsteadiness parameter increases the skin friction coefficient and the local Nusslet number. Saleh (2007) studied the flow and heat transfer of two dimensional electrically conducting viscous fluid on a continuously stretching surface in the presence of suction/blowing with variable viscosity and thermal conductivity. Samad and Mohebujjaman (2009) studied a steady-state two dimensional magneto hydrodynamic heats and mass transfer free convection flow along a vertical stretching sheet in the presence of a magnetic field with heat generation. Fadzilah et al. (2011) studied the steady magneto-hydrodynamic boundary layer flow and heat transfer of a viscous and electrically

conducting fluid over a stretching sheet with an induced magnetic field. The results of their study show that the velocity and induced magnetic field increase with an increase in the applied magnetic field.

The problem of heat transfer from boundary layer flow driven by a continuous moving surface is of importance in a number of industrial manufacturing processes. Several authors have been analysed in various aspects of the pioneering work of Sakiadis (1931). Crane (1970) have investigated the steady boundary layer flow due to stretching with linear velocity. Vlegaar et al. (1977) have analysed the stretching problem with constant surface temperature and Soundalgekar et al. (1980) have analysed the constant surface velocity.

Hashim et al. (2003) applied Adomian decomposition method to the classical Blasius equation. Wazwaz (1997) used Adomian decomposition method to solve the boundary layer equation of viscous flow due to a moving sheet. Awang Kechil and Hashim (2009) used Adomian decomposition method to get the approximate analytical solution of an unsteady boundary layer problem over an impulsively stretching sheet.

Awang Kechil and Hashim (2009) applied Adomian decomposition method to a two by two system of nonlinear ordinary differential equations of free-convective boundary layer equation. Hayat et al. (2009) analysed the MHD flow over a nonlinearly stretching sheet by employing the Modified Adomian decomposition method.

II . FORMULATION OF THE PROBLEM

The formulation of the problem presented by Wubshet Ibrahim et al. (2012) is described below.

Consider the unsteady two-dimensional laminar boundary layer flow of an incompressible fluid moving over a continuously stretching sheet immersed in an incompressible electrically conducting fluid with heat source or sink. The flow is subjected to a transverse magnetic field of strength B which is

assumed to be applied in the positive y -direction, normal to the surface. We also assume that the sheet is stretched

With the stretching velocity $U_w(x, t^*) = \frac{ax}{1-\gamma t^*}$ along the x axis. The surface temperature of the sheet is $T_w(x, t^*) = T_\infty + \frac{bx}{1-\gamma t^*}$ and the transverse unsteady magnetic field strength applied to the sheet is $B(t^*) = \frac{B_0}{\sqrt{1-\gamma t^*}}$. Where a , b and γ are constants, $a \geq 0$, $b \geq 0$, $\gamma \geq 0$ and $\gamma t^* \leq 1$, time is denoted by t^*

Both a and γ have dimension $(\text{time})^{-1}$. T_∞ is ambient temperature, B_0 is constant magnetic field. Under these assumptions, along with the boundary-layer approximations, the unsteady boundary layer equations governing the flow and heat transfer as it was given by Elbashbeshy (2010).

The basic boundary layer equations that govern momentum and energy respectively are

$$\frac{\partial u}{\partial x} + \frac{\partial v}{\partial y} = 0 \quad (2.1)$$

$$\frac{\partial u}{\partial t^*} + u \frac{\partial u}{\partial x} + v \frac{\partial u}{\partial y} = \nu \frac{\partial^2 u}{\partial y^2} - \sigma \frac{\beta^2 u}{\rho} \quad (2.2)$$

$$\frac{\partial T}{\partial t^*} + u \frac{\partial T}{\partial x} + v \frac{\partial T}{\partial y} = \alpha \frac{\partial^2 T}{\partial y^2} + \frac{Q}{\rho c_p} (T - T_\infty) \quad (2.3)$$

subject to the boundary conditions

$$\begin{aligned} y = 0 : u &= u_w(x, t^*), & v &= 0, T(x, t^*) = T_w(x, t) \\ y \rightarrow \infty : u &= 0, & T &= T_\infty \end{aligned} \quad (2.4)$$

where u and v are the velocity components in the x and y directions respectively, T is the fluid temperature inside the boundary layer, t is the time, k is the thermal conductivity, ν is the kinematics viscosity, c_p is the specific heat at constant pressure, ρ is the density, $Q > 0$ represents a heat source and $Q < 0$ represents a heat sink, T_∞ is the temperature far away from the stretching sheet.

The equation of continuity is satisfied if we choose a stream function $\psi(x, y)$ such that

$$u = \frac{\partial \psi}{\partial y}, \quad v = \frac{-\partial \psi}{\partial x}.$$

The mathematical analysis of the problem is simplified by introducing the following dimensionless similarity variables:

$$\eta = \sqrt{\frac{a}{v(1-\gamma t^*)}} y$$

$$\psi(x, y) = \sqrt{\frac{avx}{(1-\gamma t^*)}} f(\eta) \quad (2.5)$$

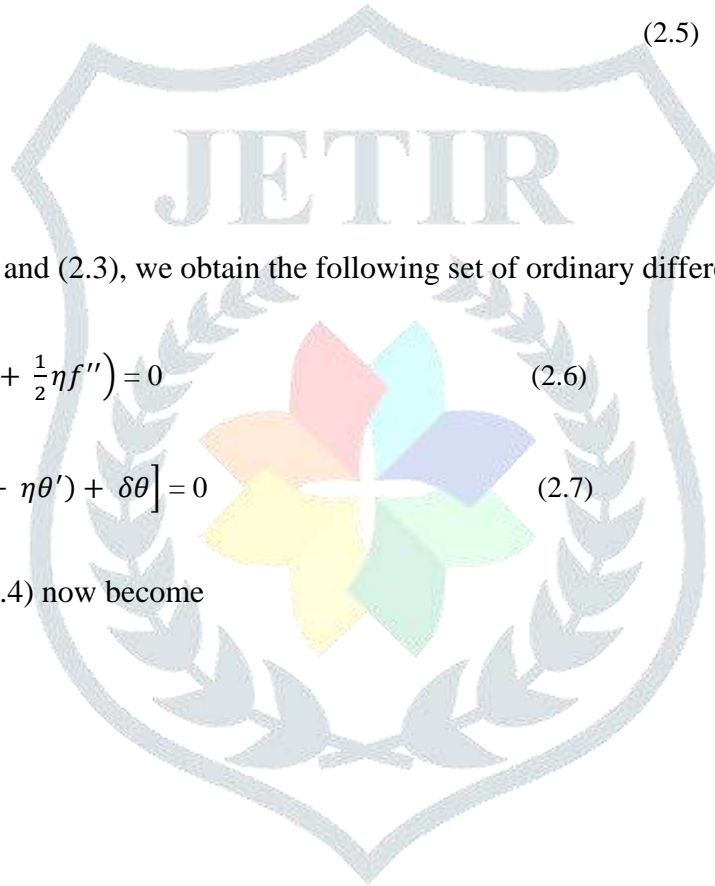
$$\theta(\eta) = \frac{T-T_0}{T_w-T_\infty}$$

Substituting (2.5) into (2.2) and (2.3), we obtain the following set of ordinary differential equations:

$$f''' + ff'' - f'^2 - Mf' - A\left(f' + \frac{1}{2}\eta f''\right) = 0 \quad (2.6)$$

$$\theta'' + Pr \left[f\theta' - f'\theta - \frac{A}{2}(\theta + \eta\theta') + \delta\theta \right] = 0 \quad (2.7)$$

The boundary conditions (2.4) now become



$$\begin{aligned} \eta = 0: & \quad f = 0, & \quad f' = 1, & \quad \theta = 1 \\ \eta \rightarrow \infty: & \quad f' = 0, & \quad \theta = 0 \end{aligned} \quad (2.8)$$

where the primes denote differentiation with respect to η , $A = \frac{\gamma}{\alpha}$ is a parameter that measures the unsteadiness, $Pr = \frac{\mu C_p}{k}$ is the prandtl number (μ is the viscosity),

$\delta = \frac{Q_k Re_x}{\mu C_p Re_k^2}$ is the dimensionless heat source or sink parameter, $Re_x = \frac{U_w x}{\nu}$ is the local Reynolds number, $M = \frac{\sigma(B_0)^2}{\rho \alpha}$ is the magnetic parameter and $Re_x = \frac{U_w \sqrt{k}}{\nu}$. The physical quantities of interest in this problem are the skin friction coefficient C_f and the local Nusselt number Nu_x which are defined as

$$C_f = \frac{\mu \left(\frac{\partial u}{\partial y} \right)_{y=0}}{[\rho U_w^2 / 2]}, \quad Nu_x = \frac{-x \left(\frac{\partial T}{\partial y} \right)_{y=0}}{T_w - T_\infty}$$

$C_f \sqrt{Re_x} = f''(0)$, $\frac{Nu_x}{\sqrt{Re_x}} = -\frac{1}{\theta(0)}$ where $Re_x = \frac{x U_w}{\nu}$ is the local Reynolds number based on the surface velocity.

III. ANALYTIC SOLUTION

The analytic solution for the above coupled ordinary differential Eqs. (2.6) and (2.7) for different values of unsteadiness parameter A , magnetic parameter M , heat source or sink parameter δ and Prandtl number Pr is obtained using Adomian decomposition method and homotopy perturbation method with Padé approximants.

3.1 FUZZY ADOMIAN DECOMPOSITION METHOD

Using Adomian decomposition method, rearranging (2.3) and (2.7) as follows

$$f''' = -ff'' + f'^2 + Mf' + A\left(f' + \frac{1}{2}\eta f''\right) \quad (3.1)$$

$$\theta'' = -\text{Pr}\left[f\theta' - f'\theta - \frac{A}{2}(\theta + \eta\theta') + \delta\theta\right] \quad (3.2)$$

While applying the standard procedure of ADM

Eqs (3.1) and (3.2) becomes

$$L_1 f = \left(-ff'' + f'^2 + Mf' + A\left(f' + \frac{1}{2}\eta f''\right)\right) \quad (3.3)$$

$$L_2 \theta = -\text{Pr}\left([f\theta' - f'\theta - \frac{A}{2}(\theta + \eta\theta') + \delta\theta]\right) \quad (3.4)$$

Where

$$L_1^{-1}(\cdot) = \int_0^\eta \int_0^\eta \int_0^\eta (\cdot) d\eta d\eta d\eta \quad \text{and} \quad L_2^{-1}(\cdot) = \int_0^\eta \int_0^\eta (\cdot) d\eta d\eta$$

Applying the inverse operator on both sides of (3.3) and (3.4)

$$L_1^{-1} L_1 f = L_1^{-1} \left(-ff'' + f'^2 + Mf' + A\left(f' + \frac{1}{2}\eta f''\right)\right) \quad (3.5)$$

$$L_2^{-1} L_2 \theta = -\text{Pr} L_2^{-1} \left([f\theta' - f'\theta - \frac{A}{2}(\theta + \eta\theta') + \delta\theta]\right) \quad (3.6)$$

Simplify eqs (3.5) and (3.6) we get

$$f(\eta) = \eta + \frac{\alpha_1 \eta^2}{2} + \int_0^\eta \int_0^\eta \int_0^\eta \left[-N_1(f) + N_2(f) + Mf' + A \left(f' + \frac{1}{2} \eta f'' \right) \right] d\eta d\eta d\eta \tag{3.7}$$

And

$$\theta(\eta) = \alpha_2 - \eta - \text{Pr} \int_0^\eta \int_0^\eta \left[N_3(f, \theta) - N_4(f, \theta) + -\frac{A}{2}(\theta + \eta\theta') + \delta\theta \right] d\eta d\eta \tag{3.8}$$

Where $\alpha_1 = f''(0)$ and $\alpha_2 = \theta(0)$ are to be determined from the boundary conditions at infinity in (2.8). The nonlinear terms $f'', f'^2, f\theta'$ and $f'\theta$ can be decomposed as Adomian polynomials $\sum_{n=0}^\infty B_n, \sum_{n=0}^\infty C_n, \sum_{n=0}^\infty D_n$ and $\sum_{n=0}^\infty E_n$ as follows

$$N_1(f) = \sum_{n=0}^\infty B_n = ff'' \tag{3.9}$$

$$N_2(f) = \sum_{n=0}^\infty C_n = (f')^2 \tag{3.10}$$

$$N_3(f, \theta) = \sum_{n=0}^\infty D_n = f\theta' \tag{3.11}$$

$$N_4(f, \theta) = \sum_{n=0}^\infty E_n = f\theta' \tag{3.12}$$

Where $B_n(f_0, f_1, \dots, f_n)$ $C_n(f_0, f_1, \dots, f_n)$ and $D_n(f_0, f_1, \dots, f_n, \theta_0, \theta_1, \dots, \theta_n)$

$E_n(f_0, f_1, \dots, f_n, \theta_0, \theta_1, \dots, \theta_n)$ are the so called Adomian polynomials. In the Adomian decomposition method (1983) f and θ can be expanded as the infinite series

$$f(\eta) = \sum_{n=0}^\infty f_n = f_0 + f_1 + f_2 + \dots + f_m + \dots$$

$$\theta(\eta) = \sum_{n=0}^{\infty} \theta_n = \theta_0 + \theta_1 + \theta_2 + \dots + \theta_m + \dots \quad (3.13)$$

Substituting (3.9),(3.10),(3.11) and (3.12) into (3.7) and (3.5) gives

$$\sum_{n=0}^{\infty} f_n(\eta) = \eta + \frac{\alpha_1 \eta^2}{2} + \int_0^\eta \int_0^\eta \int_0^\eta \left[-\sum_{n=0}^{\infty} B_n + \sum_{n=0}^{\infty} C_n + M \sum_{n=0}^{\infty} f_n' + A \sum_{n=0}^{\infty} \left(f_n' + \frac{1}{2} \eta f_n'' \right) \right] d\eta d\eta d\eta \quad (3.14)$$

And

$$\sum_{n=0}^{\infty} \theta_n(\eta) = \alpha_2 - \eta - \text{Pr} \int_0^\eta \int_0^\eta \left[\sum_{n=0}^{\infty} D_n - \sum_{n=0}^{\infty} E_n - \frac{A}{2} \sum_{n=0}^{\infty} (\theta_n + \eta \theta_n'') + \delta \theta_n \right] d\eta d\eta \quad (3.15)$$

Hence, the individual terms of the Adomian series solution of the equation (2.3)–(2.C8) are provided below by the simple recursive algorithm

$$f_0(\eta) = \eta + \frac{\alpha_1 \eta^2}{2} \quad (3.16)$$

$$\theta_0(\eta) = \alpha_2 - \eta \quad (3.17)$$

$$f_{n+1}(\eta) = \int_0^\eta \int_0^\eta \int_0^\eta \left[-B_n + C_n + M f_n' + A \left(f_n' + \frac{1}{2} \eta f_n'' \right) \right] d\eta d\eta d\eta \quad (3.18)$$

$$\theta_{n+1}(\eta) = -\text{Pr} \int_0^\eta \int_0^\eta \left[D_n - E_n + -\frac{A}{2} (\theta_n + \eta \theta_n'') + \delta \theta \right] d\eta d\eta \quad (3.19)$$

For practical numerical computation, we take the m-term approximation of $f(\eta)$ and

$$\theta(\eta) \text{ as } \phi_m(\eta) = \sum_{n=0}^{m-1} f_n(\eta) \text{ and } \omega_m(\eta) = \sum_{n=0}^{m-1} \theta_n(\eta)$$

IV. RESULTS ANALYSIS

The recursive algorithms (3.16)–(3.19) are programmed in MATLAB. We have obtained upto 15th term of approximations to both $f(\eta)$ and $\theta(\eta)$. We provided below only first few terms due to lack of space.

$$f_0 = \eta + \frac{\alpha_1 \eta^2}{2}$$

$$f_1 = \left(\frac{A}{6} + \frac{1}{6}\right) \eta^3 + \left(\frac{A\alpha_1}{16} + \frac{\alpha_1}{24}\right) \eta^4 + \left(\frac{\alpha_1^2}{120}\right) \eta^5$$

$$f_2 = \left(\frac{-\alpha_1^3}{40320}\right) \eta^8 + \left(\frac{\alpha_1^2 A}{1120} - \frac{\alpha_1^2}{5040}\right) \eta^7 + \left(\frac{\alpha_1 A^2}{192} + \frac{\alpha_1 A}{240} + \frac{\alpha_1}{720}\right) \eta^6 + \left(\frac{A^2}{60} + \frac{A}{60}\right) \eta^5$$

And

$$\theta_0 = \alpha_2 - \eta$$

$$\theta_1 = \Pr \left[\left(\frac{2\alpha_2 + A\alpha_2 - 2\alpha_2 \delta}{4} \right) \eta^2 + \left(\frac{\delta - A + \alpha_1 \alpha_2}{6} \right) \eta^3 - \left(\frac{\alpha_1}{24} \right) \eta^4 \right]$$

$$\begin{aligned} \theta_2 = & \Pr \left(\frac{\alpha_2}{24} + \frac{A\alpha_2}{24} - \frac{Pr\alpha_2}{24} + \frac{APr\alpha_2}{24} + \frac{A^2 Pr\alpha_2}{32} + \frac{Pr\alpha_2 \delta^2}{24} - \frac{APr\alpha_2 \delta}{12} \right) \eta^4 - \\ & \Pr \left(\frac{A}{60} + \frac{Pr\delta}{60} - \frac{\alpha_1 \alpha_2}{120} + \frac{A^2 Pr}{60} + \frac{Pr\delta^2}{120} - \frac{APr}{60} - \frac{APr\delta}{40} - \frac{A\alpha_1 \alpha_2}{80} \right. \\ & \left. \frac{Pr\alpha_1 \alpha_2}{60} - \frac{APr\alpha_1 \alpha_2}{60} + \frac{Pr\alpha_1 \alpha_2 \delta}{120} + \frac{1}{60} \right) \eta^5 \\ & - \Pr \left(\frac{-\alpha_1}{240} + \frac{A\alpha_1}{160} - \frac{Pr\alpha_1}{240} - \frac{\alpha_1^2 \alpha_2}{720} + \frac{APr\alpha_1}{1440} + \frac{Pr\alpha_1 \delta}{720} + \frac{Pr\alpha_1^2 \alpha_2}{360} \right) \eta^6 + \\ & \left(\frac{Pr\alpha_1^2}{1008} - \frac{\alpha_1^2}{1260} \right) \eta^7 \end{aligned}$$

The undetermined values of α_1 and α_2 are computed using the boundary condition at infinity in (2.8). The difficulty at infinity is tackled by applying the diagonal Padé approximants Boyd (1997) that approximate $f'(\eta)$ and $\theta(\eta)$ using $\phi'_{15}(\eta)$ and $\omega_{15}(\eta)$ applying infinity to the diagonal Padé approximants [N/N] that approximates $f'(\eta)$ and $\theta(\eta)$ ranging of N from 2 to 10 provides a two by two system of non linear algebraic equation, then obtained nonlinear system are solved by employing Newton Raphson method.

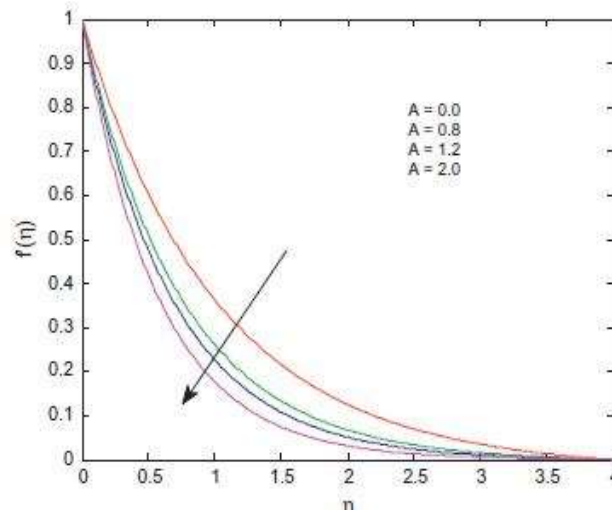


Fig.1. Velocity for different values of A, when $M = 1$, $\delta = 1$, and $Pr = 1$.

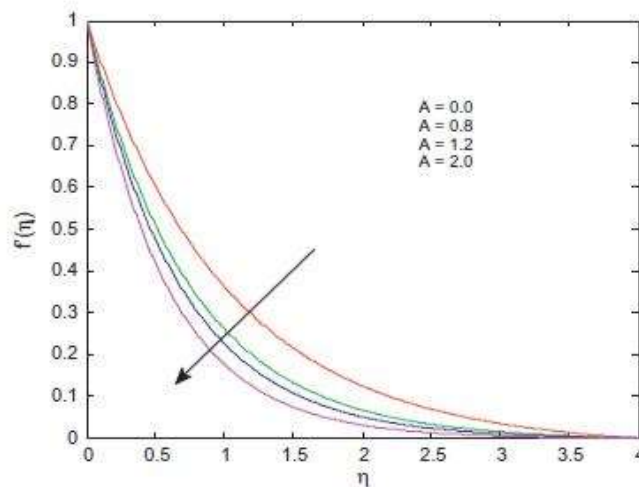


Fig.2. Velocity graph for different values of A, when $M = 1$, $\delta = 0$, and $Pr = 0.72$

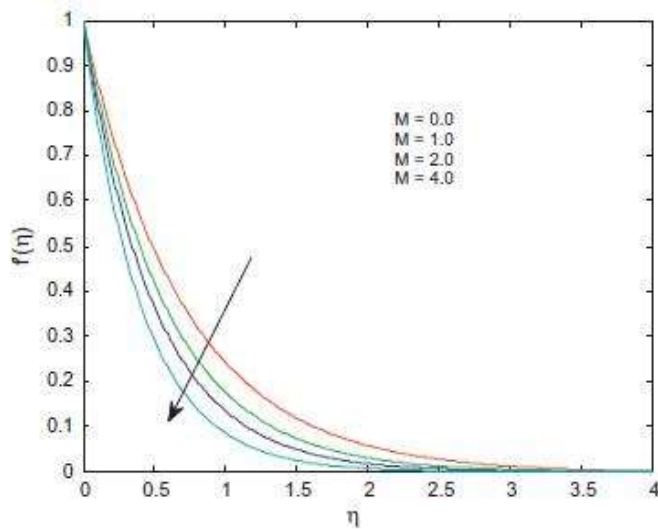


Fig.3. Velocity graph for different values of M , when $A = 1$, $\delta = 1$, and $Pr = 0.72$.

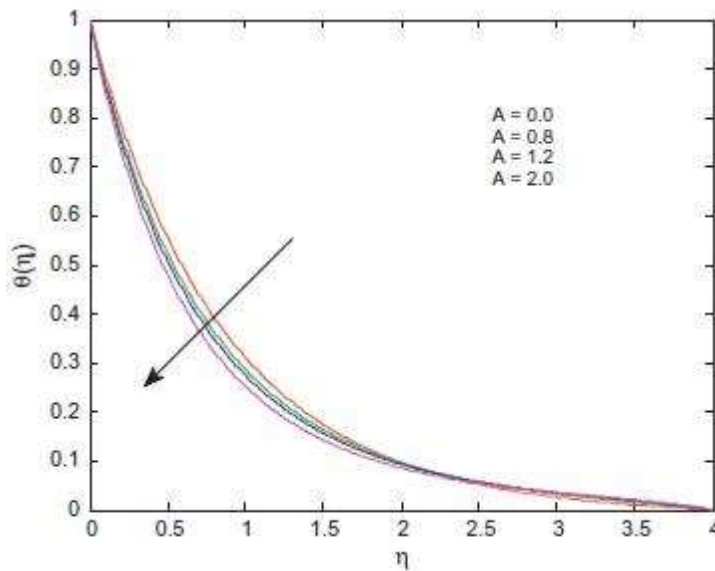


Fig.4. Temperature graph for different values of A , when $M = 1$, $\delta = -1$, and $Pr = 0.72$.

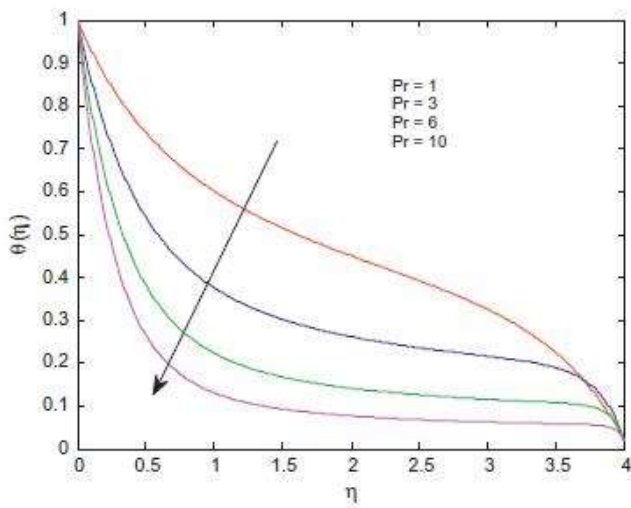


Fig.5. Temperature graph for different values of Pr, when $M = 1$, $\delta = 1$, and $A = 1.2$.

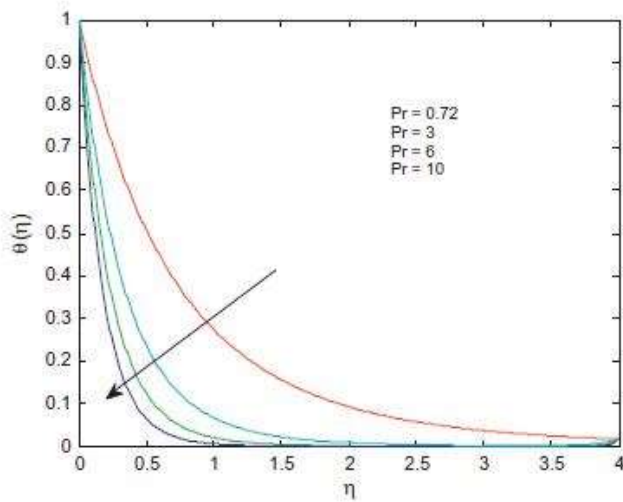


Fig.6. Temperature graph for different values of Pr, when $M = 1$, $\delta = -1$, and $A = 1.2$.

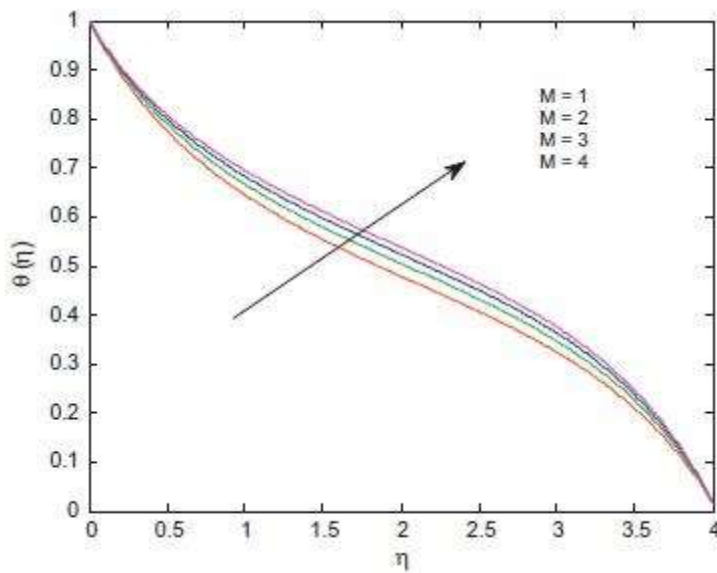


Fig.7. Temperature graph for different values of M , when $Pr = 0.72$, $\delta = 1$, and $A = 1.2$.

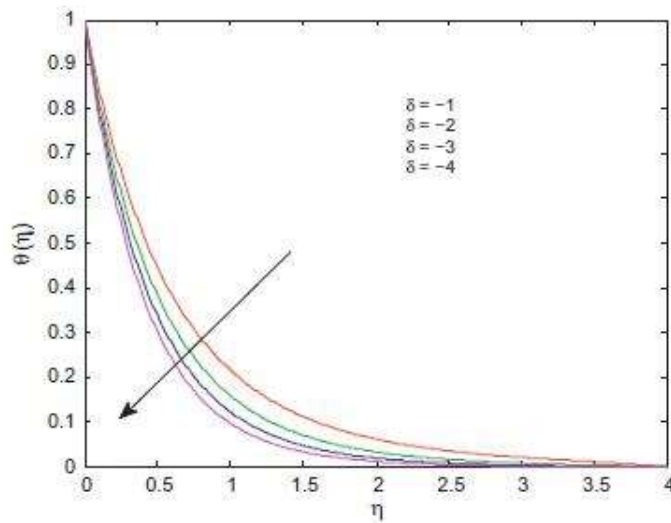


Fig.8. Temperature graph for different values of δ , for the case of heat sink when

$A = 1.2$, $M = 1$, and $Pr = 1$.

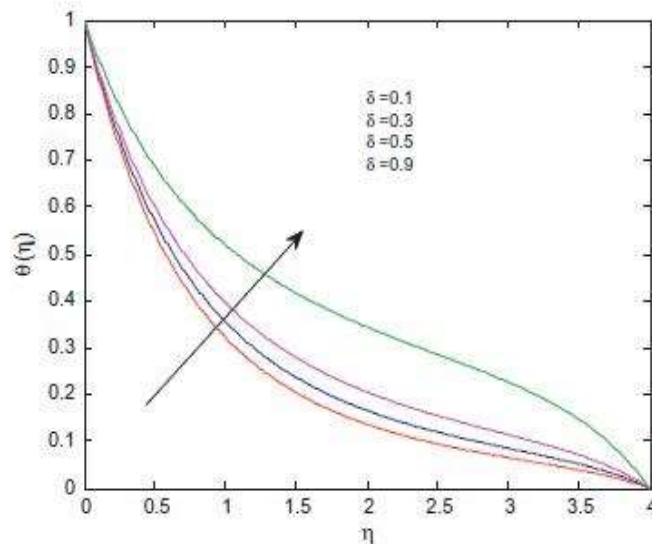


Fig.9. Temperature graph for different values of δ , for the case of heat source when

$A = 1.2$, $M = 1$, and $Pr = 1$.

Figs. 1–3 show the velocity graphs for different values of A and M , respectively, when the other parameters are fixed. Figs. 1 and 2 indicate that the velocity graph decreases as the unsteadiness parameters increase. This is due to the fact that the velocity boundary layer thickness decreases as unsteadiness parameter A increases. This results in the reduction of velocity graph. Fig. 3 reveals the influence of magnetic parameter M on flow field. It is observed that flow velocity decreases with an increase in the magnetic characteristic. Moreover, the velocity approaches to zero as the distance from the sheet increases. The similarity solution for the dimensionless velocity in Figs. 2–4 also shows that the velocity boundary layer thickness decreases monotonically when unsteadiness parameter A and magnetic parameter M increases. Moreover, the graphs show that velocity gradient on the surface of a stretching sheet increases with an increase in both parameters A and M .

Figs. 5–9 represent the variation of temperature with respect to the governing parameters, namely, unsteadiness parameter A , magnetic parameter M , heat source or sink parameter δ and Prandtl number Pr . Fig. 5 shows that the variation of temperature with respect to unsteadiness parameter A when the other parameters are fixed. It shows that the temperature decreases as the values of parameter A increases. This is due to the fact the heat transfer rate increases with an increase in unsteadiness parameters. This leads to a reduction in temperature. Figs. 3, 7 represent the variation of temperature with respect to Prandtl number Pr for both heat source and sink. The graphs show that the temperature graph decreases when the values of Prandtl number Pr increase. This is due to the fact that a higher Prandtl number fluid has relatively low thermal conductivity, which reduce the conduction and thermal boundary layer thickness and as a result a temperature decrease. From the graph it is possible to see that thermal boundary layer thickness for heat source is thicker than heat sink.

Fig. 7 represents the variation of temperature with respect to magnetic parameter M when other parameters are fixed. It reveals that the temperature decreases with an increase of magnetic parameter. This is due to additional work expended in dragging the fluid in the boundary layer against the action of the Lorentz force and energy is dissipated as thermal energy which heats the fluid. This induces a rise in temperature. Furthermore, the graph shows that the thermal boundary-layer thickness slightly increases with an increase in magnetic parameter M . Fig. 8 shows the variation of temperature with respect to heat sink while other parameters are fixed. When heat sink increases more heat removed from the

sheet which reduces the thermal boundary-layer thickness. This reduce the temperature of the sheet.

Fig. 9 illustrates the variation of temperature with respect to heat source. It is observed that when heat source increases the temperature is increases. This due to the fact that heat source can add more heat to the stretching sheet which increases its temperature. This increases the thermal boundary layer thickness. In order to check the accuracy of the numerical solutions, a comparison of heat transfer at the surface for different values of A and Pr are made with Elbashbeshy (2010).

V. COCLUSION

Fuzzy Adomian decomposition method and Fuzzy homotopy perturbation method have been employed to study unsteady MHD boundary-layer flow and heat transfer due to stretching sheet in the presence of heat source or sink. The effects of the various governing parameters on the heat transfer characteristic were examined.

The numerical results of this study show that the skin friction coefficient is in good agreement with those obtained by previous investigators in the absence of magnetic parameter, heat source or sink d and unsteadiness parameter Pr . The result obtained by this method is more reliable than previous results Wubshet Ibrahim et al. (2012). Moreover, the graphs show more physical reality than the previous paper. Briefly the above discussion can be summarized as follows:

1. Both the velocity and temperature graphs decrease as unsteadiness parameters increase.
2. The thickness of velocity boundary layer decreases with an increase in unsteadiness and magnetic parameter.
3. The temperature decreases with an increase in the value of the unsteadiness parameter A , magnetic parameter M , heat source or sink parameter δ and Prandtl number Pr .
4. The thickness of thermal boundary layer decreases with increase in both unsteadiness and Prandtl number parameters and opposite result observed for magnetic parameter.
5. An increment in unsteadiness parameter A increases both the skin friction coefficients and local Nusselt number.
3. An increase in magnetic parameter M increases the skin friction coefficient.
7. An increment in heat source or sink reduces the local Nusselt number.
8. As the values of Prandtl number increase, the local Nusselt number also increases.
9. The wall temperature gradient decreases with increasing unsteadiness parameter and Prandtl number.

BIBLIOGRAPHY

- [1] Abassy, T.A. (2010), Improved Adomian decomposition method, Computers and Mathematics with Applications, Vol. 59 No. 1, pp. 42-54.
- [2] Abassy, T.A, Magdy A. El-Tawil, Hassan K. Saleh (2007) The solution of Burgers and good Boussinesq equations using ADM–Padé technique, Chaos, Solitons and Fractals Vol 32 pp 1008–1026.

- [3] Abbaoui, K. and Cherruault, Y. (1994), Convergence of Adomian method applied to differential equations, Computers and Mathematics with Applications, Vol. 28 No. 5, pp. 103-9.
- [4] Abbaoui, K. and Cherruault, Y. (1994b), Convergence of Adomian method applied to nonlinear equations, Mathematical and Computer Modelling, Vol. 20 No. 9, pp. 60-73.
- [5] Abbaoui, K. and Y. Cherruault, (1995) New ideas for proving convergence of decomposition method, Computer and Mathematical Application. 29 103-108.
- [6] Abbasbandy, S. (2005), Extended Newton's method for a system of nonlinear equations by modified Adomian decomposition method. Applied Mathematics and Computation, vol 170(1) pp 648-656.
- [7] Abbasbandy, S. (2007), A numerical solution of Blasius equation by Adomian decomposition method and comparison with homotopy perturbation method. Chaos, Solitons and Fractals 31 (1), 257-280.
- [8] Abramowitz, M. and Stegun I.A. (1965) Handbook of Mathematical Functions, Dover, New York.
- [9] Achouri, T. and Omrani, K. (2009), Numerical solutions for the damped generalized regularized long-wave equation with a variable coefficient by Adomian decomposition method, Communications in Nonlinear Science and Numerical Simulation, Vol. 14 No. 5, pp. 2025-33.
- [10] Adomian, G. (1983), Stochastic Systems, Academic Press, New York, NY.
- [11] Adomian, G. (1986), Nonlinear Stochastic Operator Equations, Academic Press, Orlando, FL.
- [12] Adomian, G. (1994), Solving Frontier Problems of Physics: The Decomposition Method. Kluwer Academic Publication, Boston.

[13] Adomian, G. and R. Rach (1983), Inversion of nonlinear stochastic operators, J.

Math. Anal.Appl. pp. 3946.

[14] Adomian, G. Applications of Stochastic Systems Theory to Physics and

Engineering, Academic Press, New York, in press.

[15] Adomian, G. and R. E. Bellman, New Methods in Partial Differential Equations,

Reidel, Dordrecht, in press.

